(Received 6 July 2024, Accepted 16 August 2024, Scheduled 6 September 2024)

# Calculation and Analysis of Eddy Current Loss in High Temperature Permanent Magnet Canned Motor

Quanfeng Li[1], Ziwei Wang[1], and Xiang Li[1, 2, *]

[1]*Shanghai Dianji University, Shanghai, China*
[2]*Shanghai First Machine Tool Factory Co. Ltd, Shanghai, China*

**ABSTRACT:** As an important part of the primary circuit system of a nuclear power plant, the safe and stable operation of the canned motor of a nuclear main pump is crucial. The existence of stator can and rotor can in the air gap of a canned motor will generate additional eddy current loss during the operation of the motor, which will be detrimental to the long-term stable operation of the motor. Therefore, in this paper, in order to analyze and weaken the eddy current loss generated on the shielding can, using the empirical formula method, the eddy current loss generated by the shielding can before optimization is calculated, and the relationship among the eddy current loss, can thickness, and motor speed is derived. Subsequently, two shielding can structure optimization schemes were proposed, and the reduction of eddy current loss after optimization was calculated using finite element simulation software. The effects of different optimization schemes were compared. Finally, peak torque and current experiments are conducted on the original motor to verify the accuracy of the finite element calculation results. The results show that both optimization schemes proposed in this paper can reduce the eddy current loss, and the axial segmentation scheme has a better reduction effect on the shielding can.

## 1. INTRODUCTION

As a special motor, the high-temperature canned motor (CM) of the nuclear main pump is mainly used to pump the cooling circulating medium inside the reactor. Compared to conventional motors, CM has an extra structure in the air gap: stator can and rotor can. During the operation of the CM, the shielding can cuts the magnetic inductance and generates large eddy current loss, which causes the shielding can to overheat and even leads to the demagnetization of the permanent magnets. Therefore, it is very important to accurately calculate and optimize the eddy current loss of the shielding can.

At present, the research on the problem of eddy current loss of CM is mainly summarized in the following three aspects:

In terms of theoretical research, Yu et al. conducted detailed theoretical research on the concentration effect of eddy current, the rate of change of phase current, and the field coupling effect, and analyzed factors contributing to eddy current loss [1]. Robinson et al., Yu, and Yang developed the analytical calculation method for determining eddy current loss in shielded motors. Based on the calculations, it was concluded that the eddy current losses on the shielding can account for about 40% of the total CM losses [2–4]. The method is a common empirical formula for analytical calculation of eddy current loss of shielded can. On this basis, the relationship between the correction factor of this formula and the ratio of core length and pole arc factor is derived.

For finite element analysis, Guo examined the influence and effect of different shielding can parameters on eddy current loss values using ANSYS finite element software [5]. Li et al. and Chu proposed reducing eddy current loss by altering the structure of the shielding sleeve (layer) to address the eddy current loss in the permanent magnet protective layer of high-speed motors and the stator can of CMs, respectively. They validated their proposals through simulations using the finite element method [6, 7]. Yu et al. analyzed the effect of shielding can material on permanent magnet synchronous motors and their temperature fields. They concluded that using non-conductive materials for the stator can will effectively improve the efficiency of motors and reduce the temperature rise of the shielding can. Subsequently, they used finite element software to calculate the losses of shielding can made from different materials and derived the relationship between loss variation and the size and material properties of the shielding can [8].

For experimental studies, Uneyama et al. proposed a new method to measure the eddy current loss of the shielding can and designed a corresponding can loss measurement device [9]; Wang et al. investigated the effect of different positions of balance holes and jet holes on the temperature rise of the high-speed shielding pump in a liquid rocket engine [10], and the results showed that removing the balance holes reduced the internal temperature rise by 78%. Additionally, changing the structure of the jet hole reduced the internal temperature rise by 40%.

In recent years, scholars have conducted extensive research on CMs. However, relatively few studies have focused on the structural optimization of the shielding can, and there are few articles that systematically discuss optimization schemes for the shielding can. In summary, the main contributions of this paper are as follows:

* Corresponding author: Xiang Li (1624655879@qq.com).

1. Based on the original motor, 2D and 3D models of a permanent magnet synchronous shielded motor were established, and the eddy current loss of the shielding sleeve was analyzed using finite element software.

2. Two shielding can optimization strategies are proposed, and the suppression effect on eddy current loss through different optimization schemes is analyzed using finite element software.

3. The test motor is designed, and experiments on peak torque and current are conducted, with the results compared to the finite element results to verify the accuracy of the simulation.

## 2. ANALYTICAL CALCULATION METHOD

When the can cuts the magnetic inductance, according to the principle of electromagnetic induction, an eddy current will be generated inside it as shown in Fig. 1.

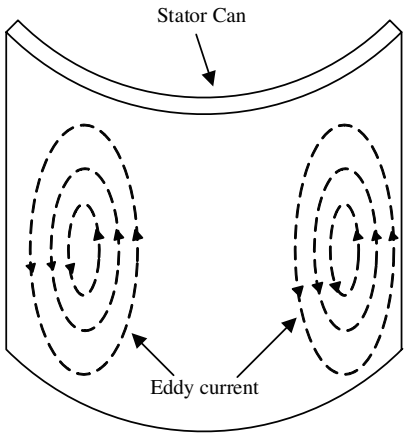


**FIGURE 1**. Schematic diagram of eddy current loss of cans.

High temperature permanent magnet CMs typically exhibit low efficiency, with an efficiency of 45.63% under rated operating conditions. The eddy current effect causes the shielded can to generate heat, resulting in an increase in the motor's internal temperature and a decrease in efficiency. Due to the motor's unique working environment, the winding component involves complex insulation design, making it challenging to optimize. However, improving the structure of the shielding can to suppress eddy current losses is feasible.

### 2.1. Math Analytic Computation Theory

Currently, the most commonly used analytical method for calculating the eddy current loss of the shielding can is the empirical formula method. This method is based on the derivation of the law of electromagnetic induction, with the calculation results subsequently corrected by a correction coefficient. This approach has the advantage of being simple and quick.

If the end resistance is ignored, the formula for calculating the eddy current loss of the shielding can is as follows

$$P = 15.5 \times \frac{B^2 L D^3 n^2 t \times 10^{-16}}{\rho} \tag{1}$$

where $B$ is the maximum value of air gap magnetic density (Gs), $L$ the core length (cm), $D$ the stator inner diameter (cm), $n$ the rotational flux revolutions per second (rps), $t$ the thickness of the shielding sleeve (cm), and $\rho$ the resistance coefficient of the shielding sleeve material (Ω-cm).

If the end resistance is considered, the equation also needs to be multiplied by a correction factor $K$. Its magnitude is related to the pole pitch and core length of the motor.

### 2.2. Analytical Calculation of Eddy Current Loss

In this study, a high-temperature permanent magnet CM produced by a company in Shanghai is analyzed. The main structural parameters of its relevant phases are shown in Table 1.

**TABLE 1**. Eddy current loss analysis calculation parameters.

| Parameters | value |
|---|---|
| Synchronous speed (rpm) | 100 |
| Thickness of can (mm) | 0.6 |
| Core length (mm) | 325 |
| Stator inner diameter (mm) | 106 |
| Coefficient of resistance of can material (Ω-cm) | $123 \times 10^{-4}$ |

Combining the above parameters, the eddy current loss $P_1$ of the stator is calculated from Equation (1) to be 3.99 W when the thickness of the shielding sleeve is 0.6 mm.

According to the empirical value, the loss of rotor can is usually about 10% of the loss of the stator can. Therefore, the total loss is:

$$P_{\text{total}} = 1.1 P_1 = 4.39\,\text{W} \tag{2}$$

Since the subsequent modeling ignores the end resistance part, the correction factor in the analytical calculation formula in this chapter is taken as 1.

## 3. FINITE ELEMENT ANALYSIS

In this paper, the motor model is constructed using ANSYS finite element software, and the stator and rotor cans are added separately. Subsequently, the vortex distribution and heat generation in the shielding can are simulated.

### 3.1. Original Motor Finite Element Calculation

In this paper, ANSYS RMxprt is used to build a permanent magnet synchronous motor, and stator and rotor cans are added in Maxwell 2D and Maxwell 3D. The 2D model and the partial enlargement are shown in Fig. 2.

Due to the high degree of symmetry of the motor, only a quarter model is used for the calculation to save computation time. Based on the actual prototype, the thickness of both the stator and rotor cans is set to 0.6 mm. The remnant magnetism $B_r$ of the permanent magnet is set to 1.1 T, and the coercivity $H_c$ is 676 kA/m.

After completing the corresponding settings, the simulation is carried out respectively for the normal motor without shielding can and CM under Maxwell's 2D transient field. The efficiencies of the two types of CMs at rated speed are calculated,

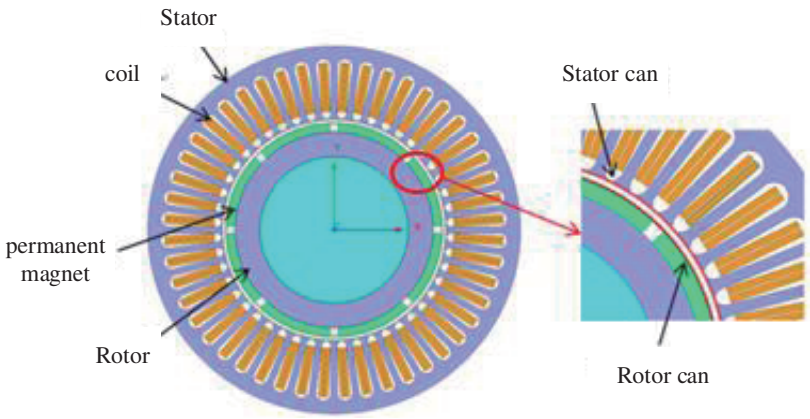


**FIGURE 2**. 2D global model and local magnification.

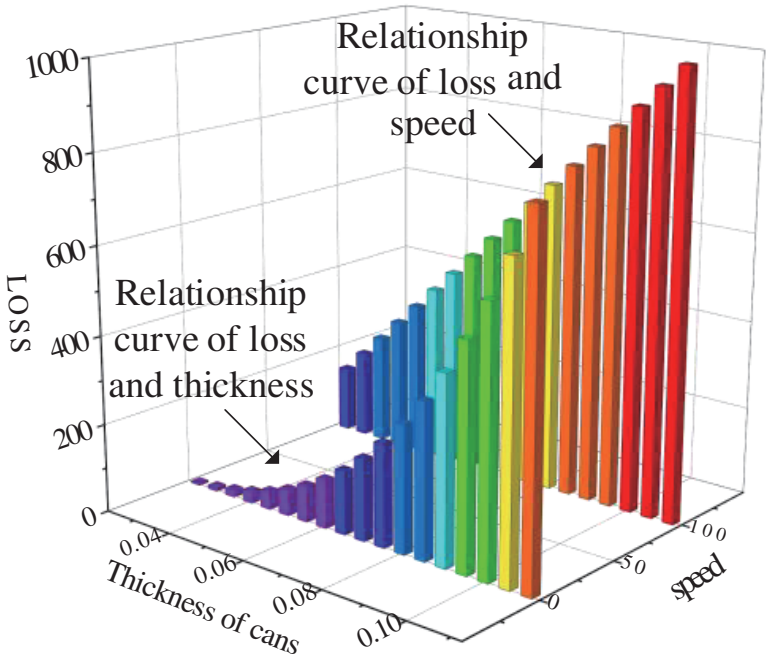


**FIGURE 3**. Finite element calculation result.

respectively, and the eddy current losses in the stator can and rotor can are calculated respectively for the CM. The simulation is carried out in one cycle. Simulation results show that the efficiency of ordinary motor at rated speed is 45.63%; the efficiency of CM is 41.79%; shielding can loss is 4.18 W.

The eddy current effect of the stator shielding can and rotor shielding can was considered, respectively. The simulation is carried out over one cycle to calculate the corresponding eddy current loss based on the thickness of the stator shielding can and the rotational speed of the CM, as shown in Fig. 3.

It is observed that the shielding can eddy current loss increases with the rotational speed and thickness of the shielding can, and it is greatly influenced by the rotational speed. Figs. 4 and 5 display the distribution of losses at the end of one cycle (0.15 s) for the rotor can and stator can at a speed of 100 rpm, respectively.

Through finite element calculations, the eddy current loss of the 0.6 mm shielding can is determined to be 4.18 W. It is observed that the eddy current loss on the stator can is significantly larger than that on the rotor can. This difference is attributed to the fact that the rotor can follows the synchronous rotation of the magnetic field. Therefore, subsequent optimization simulations will primarily focus on the stator can.

Since the rated speed of the CM in this paper is low, only 100 rpm, the calculated eddy current loss is small. However, according to Equation (1), the eddy current loss is proportional to the square of the motor rotational speed, so when the motor rotational speed becomes higher, the eddy current loss will be difficult to ignore. Therefore, this paper proposes a shielding can structure optimization strategy to achieve the purpose of suppressing the eddy current loss and improving the operation efficiency.

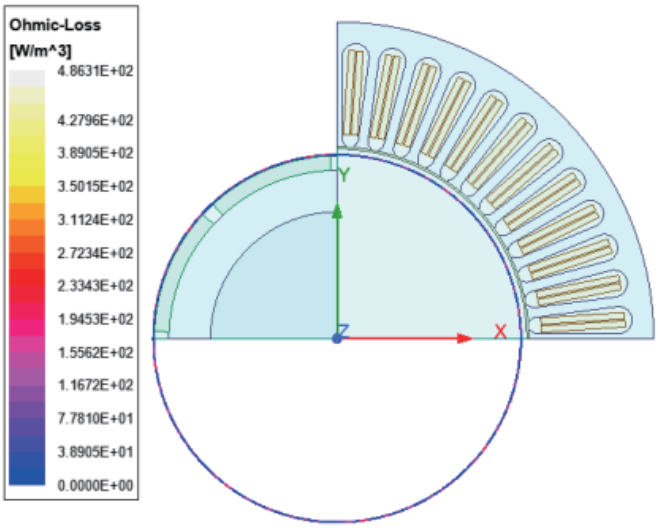


**FIGURE 4**. Rotor can loss distribution.

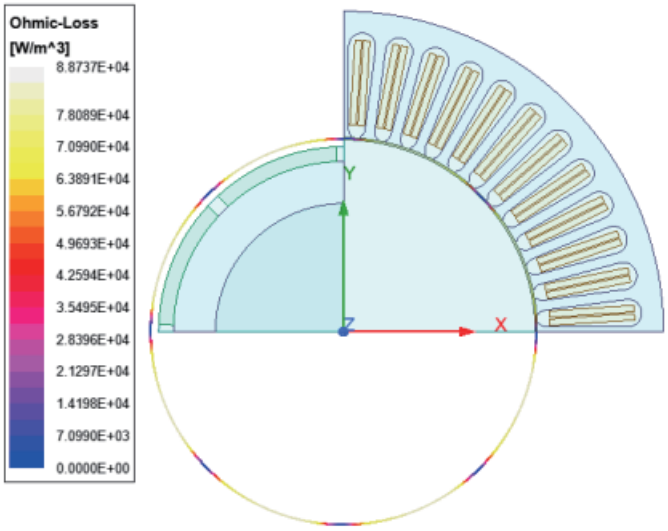


**FIGURE 5**. Stator can loss distribution.

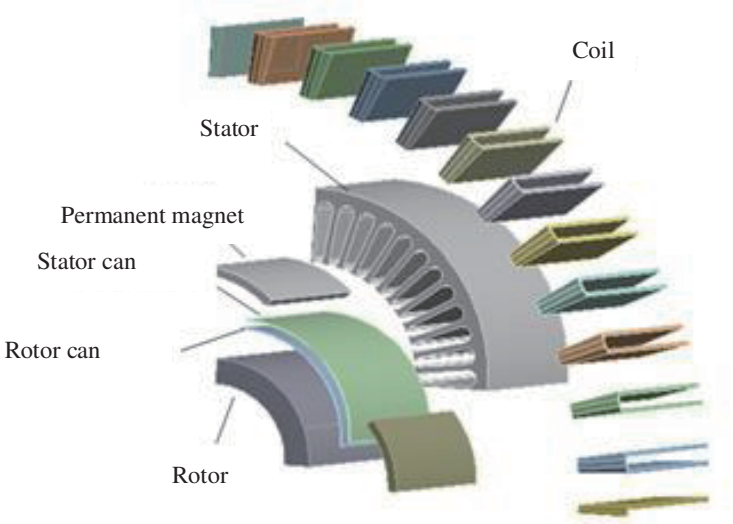


**FIGURE 6**. 3D model explosion diagram.

### 3.2. Optimized Design of Cans

To reduce the eddy current loss of the shielding can, two optimization methods are proposed in this paper: radial layering and axial segmentation. The radial layering method offers the advantage of eliminating connecting gaps on the shielding can, which avoids the risk of material leaking through the connecting gap. The advantage of axial segmentation lies in its smaller insulation area and reduced manufacturing process sensitivity to the thickness of the shielding can. Due to the structural changes in the shielding sleeve, accurately restoring the 2D model is challenging, hence the original model is reconstructed in Maxwell 3D. Fig. 6 illustrates the explosion diagram of the 3D model.

After importing the 2D model into 3D, the optimized model of the can is added to it. Fig. 7 displays the planar and three-dimensional enlarged schematic of the radial split into two layers. The morphology comprises a stack of two thinner shielding cans, with insulating connections between layers, while the total thickness remains constant.

The axial segmentation method involves dividing the can into multiple rings with a splicing structure, with insulation connections between rings. The total length remains unchanged, as illustrated in Fig. 8.

After splitting the shielding can, an insulating boundary condition is applied at the interface junction. This prevents the passage of eddy currents generated through the interface of the two conductors, simulating insulation between the conductors and confining the eddy currents to the narrow conductor after splitting. The addition of the insulating boundary condition is depicted in Fig. 9.

After completing the modeling, the remaining parameters are set to match the 2D model. The radial layering and axial segmentation of the shielding can are simulated respectively, and the resulting eddy current density distribution cloud diagrams are obtained, as shown in Figure 10. According to Fig. 10, it is

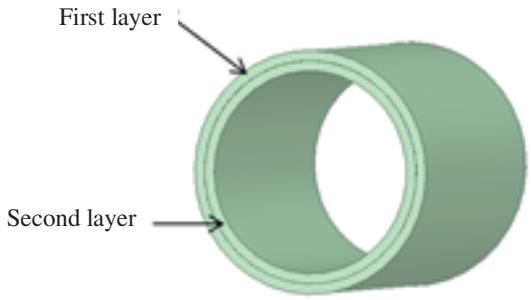


**FIGURE 7**. Radial stratification diagram.

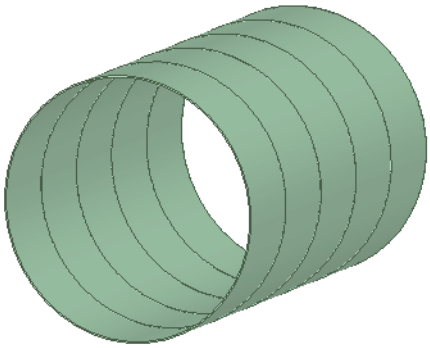

**FIGURE 8**. Axial segment diagram.

**TABLE 2**. Summary of can loss in different scheme.

| Eddy current loss in shielding cans with different splitting methods | | | |
|---|---|---|---|
| Segmentation | Segmentation Schematic | Loss | Reduction ratio |
| Radially divided into 2 layers |  | 3.28W | 21.5% |
| Radially divided into 3 layers |  | 3.248W | 22.29% |
| Radially divided into 4 layers |  | 2.961W | 29.16% |
| Radially divided into 5 layers |  | 3.027W | 27.55% |
| Axially divided into 2 segments | 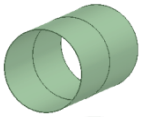 | 3.205W | 23.32% |
| Axially divided into 3 segments |  | 2.25W | 46.07% |
| Axially divided into 4 segments | 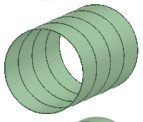 | 1.71W | 59.21% |
| Axially divided into 5 segments | 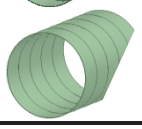 | 1.34W | 67.93% |

observed that the axial segmentation method divides the original complete eddy current loop into several smaller eddy current loops, while the radial layering method does not alter the eddy current loop.

Table 2 presents the finite element calculation results of the eddy current loss of the can for each segmentation strategy.

According to Table 2, both radial layering and axial segmentation can reduce the eddy current loss on the shielding can. The loss decreases with an increase in the number of segments. The axial segmentation method outperforms the radial layering method due to the alteration of the eddy current circuit, resulting in a more effective limitation of the eddy current loss.

**TABLE 3**. Comparison of motor efficiency before and after optimization.

| Motor type | Speed (rpm) | efficiency |
|---|---|---|
| Axially divided into 5 segments Stator inner diameter | 50 | 30.32% |
| | 100 | 45.99% |
| | 150 | 55.49% |
| | 200 | 61.79% |
| Shielding cans not optimized | 50 | 30.49% |
| | 100 | 45.63% |
| | 150 | 54.85% |
| | 200 | 60.98% |

**TABLE 4**. Peak torque simulation and experimental value.

| Speed (rpm) | Current (A) | Simulation Peak torque (Nm) | Experimental Peak torque (Nm) | Error |
|---|---|---|---|---|
| 50 | 3.47 | 9.23 | 8.36 | 9.43% |
| | 4.54 | 12.17 | 11.47 | 5.75% |
| | 5.67 | 15.28 | 14.47 | 5.30% |
| | 6.62 | 17.86 | 17.52 | 1.90% |
| | 7.55 | 20.37 | 19.60 | 3.78% |
| | 8.33 | 22.48 | 22.64 | 0.71% |
| 100 | 3.45 | 9.07 | 8.10 | 10.69% |
| | 4.54 | 11.85 | 11.59 | 2.19% |
| | 5.64 | 14.82 | 14.16 | 4.45% |
| | 6.61 | 17.51 | 16.67 | 4.80% |
| | 7.50 | 19.94 | 18.68 | 6.32% |
| | 8.29 | 22.09 | 21.77 | 1.45% |

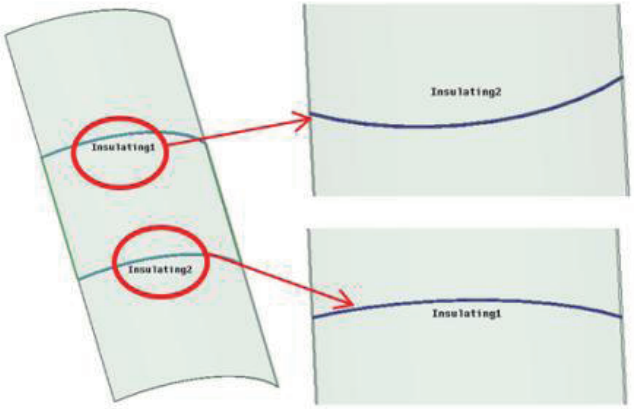


**FIGURE 9**. Setting of insulation boundary conditions.

Figure 11 illustrates the proportion of eddy current loss reduction under different optimization strategies. It is evident that when only two segments are performed on the shielding can, the effects of layering and segmentation are similar. However, when more than two segments are utilized, the attenuation effect of segmentation on eddy current loss surpasses that of layering. Nevertheless, as the number of segments increases, the degree of eddy current loss reduction diminishes.

Therefore, when various factors are considered including processing technology, if the axial length of the motor is short and not conducive to segmentation, the optimization scheme of radial segmentation into two layers can be selected. However, if the axial length is long enough, the CM can be segmented according to the actual situation to further suppress the eddy current loss.

Since the axial segmentation has the best eddy current loss suppression effect, Table 3 is obtained by calculating the efficiency of the axially segmented 5-segmented optimized motor at different speeds and the motor without CM optimization at the same speed.

It can be observed that at lower motor speeds, the optimization of the shielding sleeve does not significantly enhance the motor's efficiency. However, as the speed increases, the eddy current loss also rises, making the optimization of motor efficiency more pronounced. For instance, at a speed of 200 rpm, implementing the axial division of the 5-segment optimization scheme can improve motor efficiency by 0.8%.

It is worth noting that both optimization methods have certain drawbacks. Due to the thin thickness of the shielding can, the radial layering method is a great test for the accuracy of the processing mold. Although the axial segmentation method can more effectively suppress eddy current loss, how to ensure that the gap will not leak under the long-term operating condition

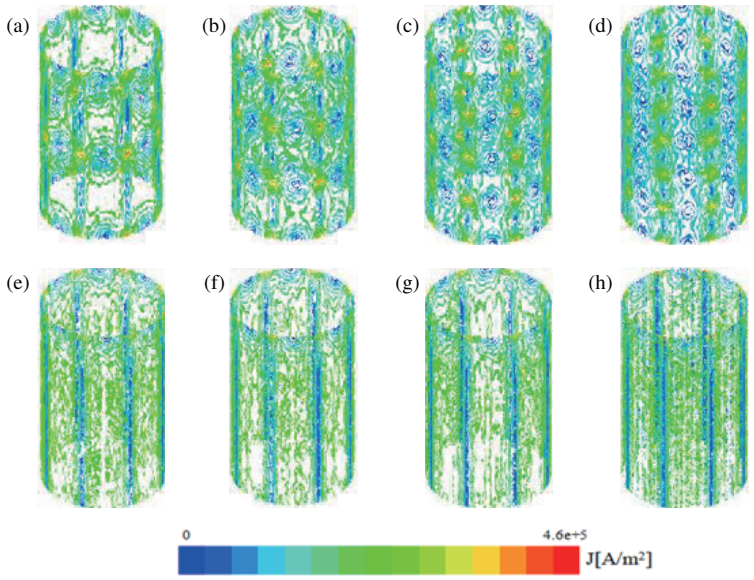


**FIGURE 10**. The stator can eddy current density distribution cloud. (a)–(d): Axially divided into 2, 3, 4 segments; (e)–(h): Radially divided into 2, 3, 4 layers.

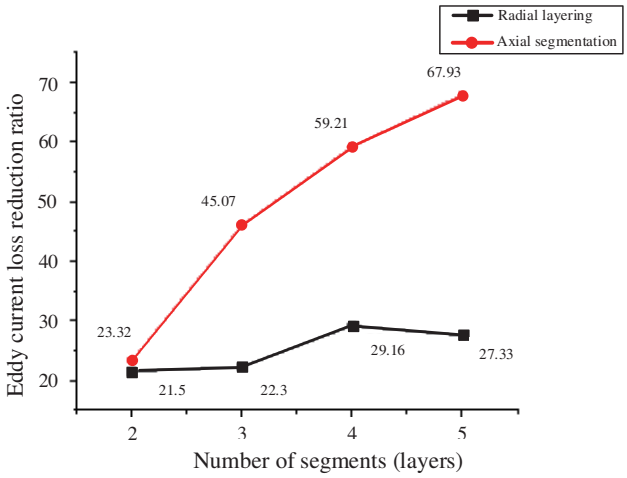


**FIGURE 11**. Reduction ratio of eddy current loss of stator can in different optimization schemes.

of the motor is a major difficulty. Overall, the axial segmentation method has higher processing difficulty and cost, but better eddy current loss suppression effect.

## 4. MOTOR EXPERIMENT

The original motor simulated in this paper is a high-temperature CM manufactured by a company in Shanghai. The experimental stand as well as the motor is shown in Fig. 12.

Since the shielding can is encapsulated in the pump, reproducing the optimized CM presented in this paper is difficult. Therefore, peak torque and current experiments were conducted on the original motor prior to optimization. The experimental results were then compared with the finite element simulation results to verify the accuracy of the simulations. The simulated and experimental results are summarized in Table 4.


**FIGURE 12**. Pictures of test benches and CM.

Based on this experimental data, the original motor model is configured to the same working conditions as the experiment and simulated in the finite element software to calculate the corresponding peak torque for current values at 50 rpm and 100 rpm, respectively. The results are then compared with the experimental values. The computational results from the finite element analysis and the experimental data are presented in Figs. 13 and 14.

By comparing the experimental and simulated data, it can be seen that the simulation results are in good agreement with the experimental calculations, thus confirming the accuracy of the simulation predictions.

Table 4 shows that there are some errors between the simulated and experimental values, which may be due to the differences between the material parameters (conductivity, permeability) and the actual material, the errors introduced by the equivalent processing of the geometrical model, and the errors caused by the meshing in the finite element simulation. The average value is taken by repeating the simulation several times and increasing the mesh quality to reduce the simulation error.

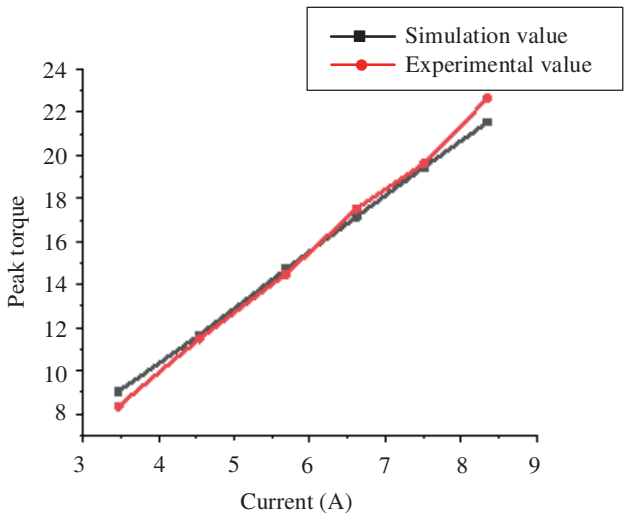


**FIGURE 13**. Comparison between simulation and experimental data of peak torque.

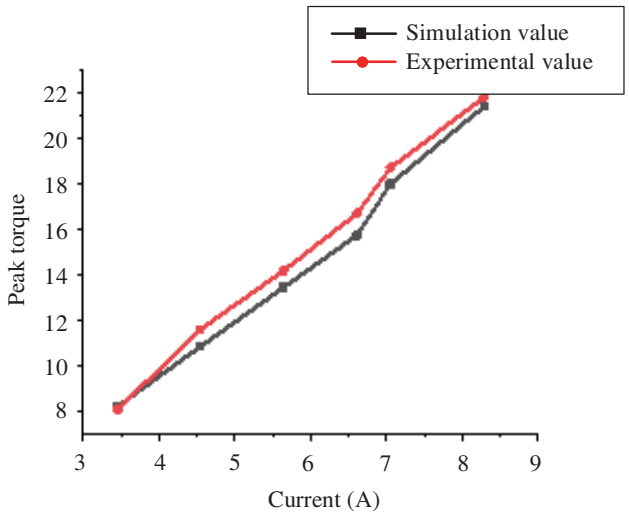


**FIGURE 14**. Comparison between simulation and experimental data of peak torque.

## 5. CONCLUSION

In this paper, the non-negligible eddy current loss generated on the stator can during the operation of the CM leads to abnormal heating of the motor, posing potential risks to its safe operation. To address this issue, optimization schemes involving radial layering and axial segmentation of the shielding can are proposed to reduce the eddy current loss. Subsequently, the efficacy of reducing eddy current loss is validated through finite element simulations, and the computational results are compared. Finally, experiments are conducted on the original prototype, and the following conclusions are drawn:

Both segmentation and layering of the shielding can will reduce eddy current loss, but the segmentation design demonstrates the most pronounced effect in suppressing eddy current loss.

From an electromagnetic performance standpoint, both radial layering and axial layering exhibit significant effects in suppressing eddy current loss. Compared with the original shielding can without segmentation, the eddy current loss of the shielding can is reduced by 29.16% and 67.93%, respectively, with radial layering and axial layering. In terms of safety, the radial layering design lacks connecting joints, thus mitigating the risk of liquid seepage into the CM after prolonged use.

Peak torque and current experiments were conducted on the original motor, and the experimental results aligned with the finite element simulation calculations. This agreement verified the accuracy of the finite element simulation calculations.

This paper does not consider changes in the conductivity of the can due to temperature changes, and the eddy current loss on the shielding can was not measured directly by experiment. This will be the focus of subsequent research.

## REFERENCES

[1] Yu, Q., C. Laudensack, and D. Gerling, "Loss analysis of a canned switched reluctance machine," in *2011 International Conference on Electrical Machines and Systems*, 1–5, Beijing, China, 2011.

[2] Robinson, R. C., I. Rowe, and L. E. Donelan, "The calculation of can losses in canned motors," *Transactions of the American Institute of Electrical Engineers. Part III: Power Apparatus and Systems*, Vol. 76, No. 3, 312–315, 1957.

[3] Yu, L., "Calculation characteristics of shielded motors," *Large motor technology*, No. 4, 24–30, 1979.

[4] Yang, T., "Finite element analysis and calculation of electromagnetic field of cage-type solid rotor canned motor," Huazhong University of Science and Technology, 2006.

[5] Guo, C., "Loss analysis and temperature rise calculation of shielded motors for nuclear power," Shenyang University of Technology, 2013.

[6] Li, W., X. Jiang, and L. Sun, "Analysis and experimental verification of rotor eddy current loss of high-speed permanent magnet motor with different canned motor structures," *Modern Machinery*, No. 3, 39–43, 2022.

[7] Chu, S., "Shielding sleeve effect and eddy current analysis of shielded permanent magnet motor," China University of Mining and Technology, 2020.

[8] Yu, T., M. Li, and S. Lun, "Study on the effect of shielding sleeve material on electromagnetic field and temperature field of shielded permanent magnet synchronous motor," *Electrical Machines and Control Applications*, Vol. 51, No. 4, 90–101, 2024.

[9] Uneyama, D., Y. Akiyama, S. Manome, and T. Naruta, "The proposal of can loss estimation method of canned motor," in *2007 International Conference on Electrical Machines and Systems (ICEMS)*, 882–885, Seoul, Korea (South), Oct. 2007.

[10] Wang, J., G. Cai, N. Yu, C. Zhou, X. Gu, and L. Cao, "Experimental study on the internal temperature rise of a high-speed canned motor pump for liquid rocket engines," *Journal of Physics: Conference Series*, Vol. 2707, No. 1, 012111, 2024.